RSC Advances

ROYAL SOCIETY OF CHEMISTRY

www.rsc.org/advances

Journal Name

ARTICLE

Characterization of water state and distribution in fibre materials by low-field nuclear magnetic resonance

Received 00th January 20xx,
Accepted 00th January 20xx

DOI: 10.1039/x0xx00000x

www.rsc.org/

Peng Ji, Jin Jin, Xianglin Chen, Chaosheng Wang, Huaping Wang

The water state and distribution in PET and cotton fibres were studied by low-field proton nuclear magnetic resonance. The spin-spin relaxation times (T_2) were measured with single pulse free induction decay (FID). There are three different states of adsorbed water in the fibre materials. The slowest fraction T_{22} can be assigned to the bulk water. The intermediate component T_{21} can be ascribed to microporous structure confined water. The fastest fraction, T_{2b}, can be assigned to the water molecules trapped by hydrogen bond owing to the chemical group. During desorption process of fibre materials, three types of water in the fibre materials work together to present the time-domain spectra, where three peaks are really related each other. Based on the interaction relationship between muti-structure of fibre materials and adsorbed water, PET fibre materials were chosen to investigate the adsorption and desorption behavior designed by copolymerization and morphology design method. The experiments of surface contact angle of fibre and fabric, moisture adsorption, water adsorption, wicking distance and water vapor permeability were carried out. The results show that the designed PET fibre materials have fast adsorption-desorption capacity. LF-NMR provides unique insight into the water state and distribution of muti-structure of fibre materials.

Introduction

An important function of textiles is supplying a maximum of wearing comfort to human bodies[1]. Clothing materials should thus have a high water retention capacity and high water transportation properties to maintain a constant temperature and humidity between skin and fabric when the human body is in a state of movement or hot environment[2-3]. When fibre materials are in service, water can be adsorbed to the materials and the interaction between water and materials has large effects on their physical properties[4-6]. At the same time, the water adsorbed to the materials exhibits a different structure from bulk water[7]. Hence, understanding the mechanism of water sorption on fibre materials may provide hints to improve not only the wearing comfort but also their textile processing[8].

Various theories have been proposed to describe the sorption mechanisms of fibre materials. Peirce introduced a model which is based on the assumption of direct and indirect sorption of water molecules on attractive groups of the materials[9]. A theory in which the interaction between water and the binding sites considers three types of water with different associating strength was proposed[10]. Langmuir developed the classical model for adsorption isotherms[11]. Young and Nelson developed a complete sorption-desorption theory, starting from the assumption of a distinct behavior of bound and condensed water (Young & Nelson)[12]. These theories have been promoted the development of fibre material, but we also find that there less experimental characterization for water state and distribution in fibre materials[13,14].

Interactions between fibre materials and water have been considered to play an important part[15,16]. Therefore, the interactions have long been a matter of extensive studies[17-20]. Many efforts have been made to investigate the states of water in the matrix by various methods, including differential scanning calorimetry (DSC)[21], Fourier transform infrared spectroscopy (FTIR)[22], NMR[23], X-ray adsorption spectra[24] etc. However, there is a clear difference of measurment results between these methods[25]. For example, it is not straightforward to interpret NIR spectra because the spectra are often very complicated owing to the overlapping of a number of overtones and combination bands in the NIR region[26]. The difficulty of monitoring the water state and distribution in fibre material lies in the fact that fibre materials have complex structure, including a combination of chemical, morphological structure[27]. Addition, most off-line measurement that typically used to monitor water state and distribution are not effective for real-time monitoring and control purposes due to a large delay[28-30].

As NMR spectroscopy reveals information about molecular structure and mobility, it became one of the most powerful non-destructive analytical tools by measuring the protons spin-spin relaxation time T_2[31]. The terms low field, intermediate field, and high field do not carry any strict meaning.

High-resolution NMR spectroscopy provides a method of structural determination for complicated molecules at magnetic field at least of 7.05 T, corresponding to 300 MHz spectrometer[32]. Low-field NMR systems equipped with permanent magnets are available for quantitative analysis in quality control, also as on-line instruments in production environments at magnetic field strengths

Key Laboratory for Modification of Chemical Fibres and Polymer Materials, College of Materials Science and Engineering, Donghua University, Shanghai 201620, P. R. China
Corresponding author1.E-mail:cswang@dhu.edu.cn, Tel: 86-021-67792960
Corresponding author2.E-mail:wanghp@dhu.edu.cn, Tel: 86-021-67792950

up to about 1 T, corresponding to 42.5 MHz ^{1}H-frequency[33].

In the recent decade, low-field nuclear magnetic resonance is attracting attention as a rapid, nondestructive and low-cost technique in the materials science[34,35]. The state and distribution of water in polymers can be determined by LF-NMR method while high-resolution NMR may destroy the mobility of water absorbed in polymer because of higher frequency pulse[36]. The state and distribution of water protons in matrix are well reflected by LF-NMR. Because of the different microenvironments that the protons experience, LF-NMR can also be regard as powerful tool to study the microstructural properties of materials matrix[37]. In general, the relaxation time of complex systems exhibits multi-component behavior, in which each component can be interpreted as representing different water states by LF-NMR method. LF-NMR measurements are successfully applied in the quality control of various types such as the water mobility and distribution in Poly (ethylene glycol)[38] and Poly (sulfobetaine methacrylate)[39].

In the present study, low-field nuclear magnetic resonance was introduced for the elucidation of water state and distribution in PET and cotton fibre materials. Based on the different relaxation time of water in fibre, the water state was proposed and the change of water state was monitored during desorption process. The water adsorption and desorption kineics in PET fibre materials designed by copolymerization and morphology design method was investigated. The results attempt to address the the water adsorption and desorption mechasim of materials with complicated structure and guide the preparation of possiblity of hydrophilic PET fibre materials by LF-NMR method.

Experimental

Materials

To distinguish between exchanging protons and non-exchanging protons, deuterium oxide (D_2O) experiments were performed. Deuterated water (D_2O) and manganese chloride used in experiments were purchased from J&K Chemical. All materials were used without further purification.

Prepartion of PETG copolymers and fibres

PETG copolymers were synthesized by macromolecular interesterification method. A representative polymerization procedure was as follows. For the esterification process, the temperature was controlled at 245 °C. The time of esterification process was about 3 hours. After which the complete removal of the anticipated produced water took place, PEG (10wt% relative to PTA) was added into the reactor, together with antimony as ethylene glycol catalyst. Polycondensation reaction occurred at the temperature 270-275 °C for 2-2.5 h.

The copolymers were designed as PETG800, PETG2000, PETG6000 and PETG20000, respectively. The samples were kept in an vacuum oven at 105 °C for 48 h. PETG copolymers were molten spinning to get the PETG fibres.

Preparation of fabrics

One hundred percent fibres 22.7 tex combed yarn was used to manufacture the fabric. The fabric was knitted in single jersey structure of 160 grams per square meter (gsm) at Jinhui New Fibre Materials Company (Suzhou, China).The fabric has the following geometrical properties: course per inch(CPI) = 48, Wales per inch (WPI) = 37, stitch length = 2.75 mm. Thecolor of the grey cotton fabric was creamy white.

Alkali reduction experiment

To investigate the relaxation time of adsorbed water by microporous structure of fibre materials, alkali reduction experiment of PET fibre materials was carried out. Cleaned and dried PET fibre dipped in 0.1 mol/L, 0.2 mol/L, 0.4 mol/L and 0.8 mol/L NaOH solution in 30 min at 90 °C, respectively. The bath ratio fo fibres to solution was 1:50. After alkali reduction treatment, the fibres were washed 5 times with deionized water, and then dried in the oven at 105 °C for 4 h.

Characterization methods

Measurement of Low field Nuclear magnetic resonance. A low field pulsed NMI 20-Analyst ((Resonance Instruments, Shanghai Niumag Corporation China) with 18.4 MHz was used in the experiment. Strip sample was placed in a 25 mm glass tube and inserted in the NMR probe. Carr-Purcell-Meiboom-Gill (CPMG) sequences were employed to measure spin-spin relaxation time, T_2. The maximum point of every second echo was accumulated using a 90° pulse of 17 μs and a 180° pulse of 34 μs. The delay between the 180° pulses, τ, was 500 μs. The amplitude of every second echo was measured, a total of 18000 points were collected, and scans were coded using a repetition time (TR) of 4 s. The relaxation measurements were performed at 32 °C.

MultiExp Inv Analysis software (Niumag Co., Ltd., Shanghai, China) was employed for data analysis. This software performs distributed exponential curve fitting. In the time domain, spin-spin relaxation data is presumed to be a sum of exponentials:

$$I_{CPMG}(t) = \sum I_m \exp(-t / T_{2m}) \quad (1)$$

T_{2m} is the relaxation times of the less mobile (said ''solid") and the mobile populations respectively. Im is the intensity of the mobile populations. The curves were then deconvoluted to Gaussian functions (each population being represented by a Gaussian) for a better schematic representation of the T_2 spectra. The intensity of peaks has been as the relative to the samples (g).

Moisture adsorption capacity. 50 g of fibre materials were kept at the condition of 20 °C and relatively humidity 65%, and then weighted the fibre (W_1) The sample was dried at 105 °C for 1 h and the sample was reweighed (W_2). The moisture adsorption (*WA*) was calculated from Eq. (2).

$$WA(\%)=(W_1 - W_2) / W_2 \times 100\% \quad (2)$$

Water adsorption capacity. 0.5 g of fibre was soaked into distilled water for 24 hours at ambient temperature. After centrifugation at 4000 g for 10 min, the weight of the fibre was measured (W_3) The sample was dried at 105 °C for 4 h and the sample was reweighed (W_4). The water retention value (*WRV*) was calculated from Eq. (3).

$$WAV(\%)=(W_3 - W_4) / W_4 \times 100\% \quad (3)$$

Surface contact angle of fibres and fabrics. The experimental procedure of surface contact angle of fibres is as follows: after being selected, the fibres were cleaned. Fibres that possess diameters between 50 μm were used. A sessile drop of water with a volume of 10 μl was vertically deposited on the sample using the equipped syringe pump and the static water CA was recorded. Then pure water was continuously and slowly pumped into the droplet at a speed of 5 μl /min until the droplet reached 20 μl, and the evolution of the water droplet was simultaneously recorded twice a second with apparent CAs calculated.

The water contact angles of fabrics were as follow: a drop of distilled water (2 μL) was placed at a rate of 0.5 μL.s^{-1} by a micro syringe. Images of the drop were recorded up to 10 s after the drop was initially set on the copolymer surface. The analysis was performed on ten different spots of the sample.

Scanning electron microscopy. SEM (Hitachi SU8010) was used to observe the microstructure of the fibres after treatment of alkali reduction experiment.

Wicking distance and diffusion time characterization of fabrics. The prepared fabrics were made in the size of 2 cm ×20 cm and one end of samples were immersed in water for 30 min to meter the height for wicking distance; The prepared fabrics were made in the size of 10 cm × 10 cm and 0.5 mL water was dropped onto the samples, then calculated the time that water spread out completely on the fabrics.

Results and discussion

Relaxation characteristic spectrum of free water.

To discuss the water mobility and distribution of fibre material/H_2O system, it is necessary for us to investigate the properties of free water without restricted effect. LF-NMR was performed by applying a radio frequency pulse to a sample within a magnetic field and assessing the relaxation properties of the proton of the sample. The inversion spectra of the T_2 of free water show only one peak, which occur at the T_2 of 2848.1 ms (shown in the *Figure 1*). The protons of free water are observed in only one status since it is a homogeneous single content.

The integrated signal intensity of the inversion spectra versus varied amounts of water is shown in *Figure 2*. The integrated signal intensity is linear with the amount of water and can directly represent all the proton numbers in each sample. The degree of fitting is 0.999, indicating that the inversion algorithm for T_2 is very reliable and accurate.

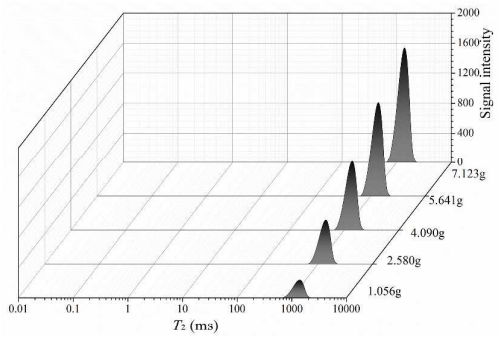

Fig. 1 T_2 inversion spectra (signal intensity versus corresponding relaxation time) for varied amounts of H_2O from 1.056 g to 7.123 g. The signal intensity represents the number of protons in the corresponding relaxation time.

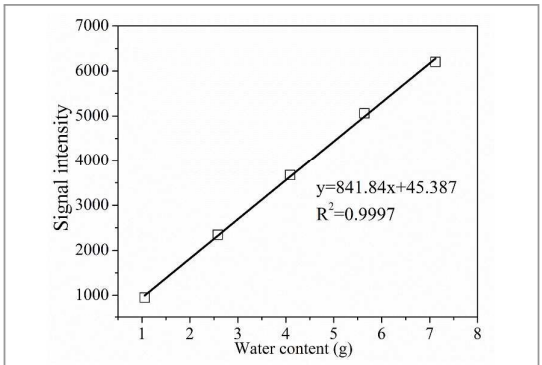

Fig. 2 The integrated signal intensity of water peak in the inversion spectrum versus the amount of H_2O.

Water mobility and distribution in fibre material/H_2O

In order to detect the mobility change of fibres mixtured with amount of water and exclude the pure water trials, D_2O was used. It is clear that there are three new protons status occurring for PET and cotton fibres mixtured with H_2O (*Figure 3*) compared with D_2O (*Figure 4*). The peaks belong to the water protons since when H_2O is replaced by D_2O. The relaxation times of three kinds of water are in the order of T_{22}>T_{21}>T_{2b}. As shown in *Figure 3*, T_{2b} was the fastest fraction, with a relaxation time of 10 ms and accounted for more than 5% of the total signal. T_{21} was the intermediate fraction (approximately 5% of the total signal) with a relaxation time of approximately 100 ms, whereas T_{22} was the slowest and had the maximum fraction, with a relaxation time of approximately 1000 ms (more than 90% of the total signal). There is a small peak occurring in *Figure 4*, which mainly comes from the small amount of H_2O left in the fibre samples. The interpretation and origin of the T_2 transverse relaxation of heterogeneous systems have been studied extensively.[40,41] In general, multiexponential relaxation behavior of various materials matrixes can be ascribed to different water fractions that exist in heterogeneous microstructures and protons of matrix.

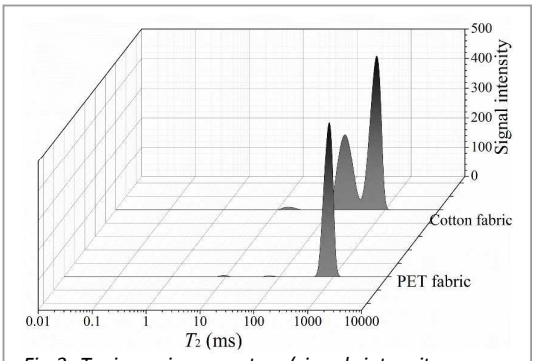

Fig.3 T_2 inversion spectra (signal intensity versus corresponding relaxation time) for H_2O/fibre mixtures after centrifugation at 4000 g for 10 min.

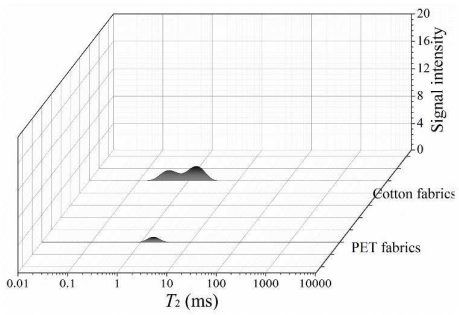

Fig.4 T_2 inversion spectra (signal intensity versus corresponding relaxation time) for D_2O/fibre mixtures after centrifugation at 4000 g for 10 min.

On the basis of the fibre material/H_2O experiment, it is reasonable to propose the origin of three proton fractions are assigned to the water molecules. Previous studies have shown that protons in fibre material systems can be differentiated into several distinct populations through their NMR relaxation behavior, which provides unique insight into the multiple structures of the fibre materials. The highest relaxation time corresponded to the most mobile population. The slowest fraction T_{22} can be assigned to the bulk water implying the T_{22} water was located in a more mobile environment. The intermediate component T_{21} can be ascribed to microporous structure confined water. The fastest fraction, T_{2b}, can be assigned to the water molecules trapped by hydrogen bond owing to the chemical group such as the -OH. To further investigate the relationship between the structures of fibre materials and relaxation behaviors and validate this assumption of relaxation times owing to the multiple structures, the T_2 of adsorption water by chemical group and microporous structure were measured. *Figure.5* shows the relaxation times of different chemical group, including the –OH, -SO_3-, -NHCO- and -COOH. We observed there is only one peak in chemical group/H_2O system although there is difference of relaxation time among these at the same mole of chemical group to water. The results of relaxation time are shown in *Table.1*. Note that T_2 (10-100 ms), this population is explained by the reason that the water is adsorped by hydrogen bond of chemical group. Due to the lack of hydrophilic adsorption group in PET fibre materials, the population of T_{2b} is less than that of cotton fibres.

Table1. The relaxation time of chemical group by LF-NMR method

Group	Molar ratio of H_2O to group	T_2'(ms)	T_2''(ms)	T_2(ms)
-OH	5:1	1.52	14.17	4.64
-SO_3Na	5:1	4.02	265.61	65.79
-COOH	5:1	57.22	75.65	65.79
-NHCO-	5:1	65.79	151.99	86.97

T_2', T_2 and T_2'' represent the start, peak and end time, respectively.

To understand the localization of T_{21}, it is informative to know the microstructure of fibre materials. The influence of morphological structure of fibre material on water state and distribution will be discussed. Compared with the populations of T_{21}, there is a distinct difference between PET and cotton fibre materials. The populations of T_{21} may be assigned to water adsorbed by the surface microstructure of fibre material. The smooth surface of PET fibre material leads the signal intensity of T_{21} less than that of cotton fibre materials. Here, to explore the relaxation time of adsorbed water by microporous structure of fibre materials, alkali reduction experiment of PET fibre materials was carried out. *Figure.6* shows the surface morphology of PET fibre materials under the condition of alkali reduction with different alkali concentration. It is clear to observe that with the increase of alkali concentration, the microporous structure of fibre materials is gradually distinct, especially at the higher alkali concentration. The PET fibre materials samples after alkali reduction treatment were used to evaluate the

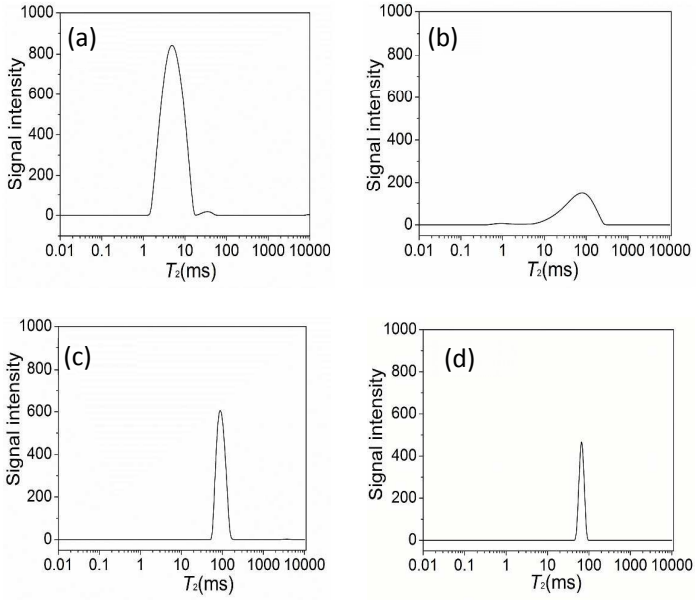

Fig.5 The relaxation times of different chemical group at the same mole of chemical group to water.

influence of microporous structure of fibre materials on the relaxation time of adsorbed water. *Figure.7* shows the population of T_{21} of PET fibre materials after alkali reduction treatment with different alkali concentration. Compared with the population of T_{21}, there is no obvious change of the signal intensity of T_{2b} and T_{22}, indicating the microporous structure of fibre materials has great effect on the population of T_{21}. With the treatment of alkali concentration increasing, the signal intensity of T_{21} increases, according to the influence of alkali concentration on the number of microporous on the surface of PET fibre materials, especially at the higher alkali concentration. It can prove that the signal intensity of T_{21} is attributed to microporous on the surface of fibre materials. From *Figure.7*, we can also get the information that with treatment of alkali concentration increasing, the relaxation time T_{21} of water adsorbed by microporous increases.

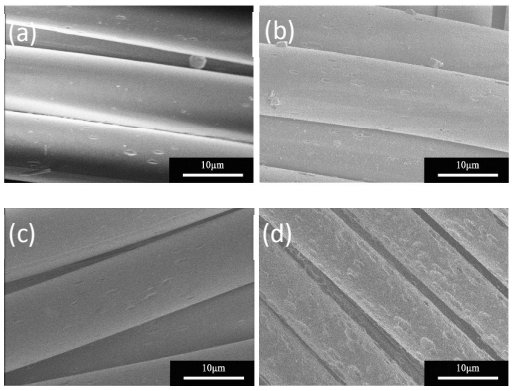

Fig.6 The surface morphology of PET fibre under the condition of alkali reduction with different alkali concentration
(a)0.1 mol/L; (b)0.2 mol/L; (c)0.4 mol/L; (d)0.8 mol/L;

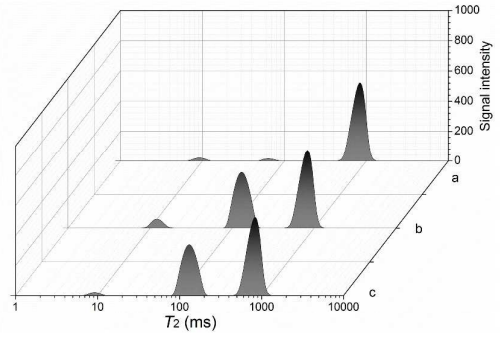

Fig.7 The population of T_{21} of PET fibre materials after alkali reduction treatment with different alkali concentration.
(a)0.1 mol/L; (b)0.2 mol/L; (c)0.4 mol/L; (d)0.8 mol/L;

Based on the analysis of T_{2b} and T_{21}, we find that T_{22} was close to that of bulk water (free water). The slowest exchangeable and highest mobile fraction, T_{22} was ascribed to mobile bulk water existing between fibres and fibres. The relaxation time of multiple structures reflects the state of adsorbed water in the fibre materials. We can conclude the order of interaction between multiple structures and water at $T'_{2b}>T'_{21}>T'_{22}$. The interaction between adsorbed water and fibre materials has large effects on its adsorption and desorption properties.

The wearing comfort of fabrics mostly lies in its adsorption and desorption properties. It is necessary for us to further investigate the influence of mobility of water adsorbed by multiple structures of fibre materials on the adsorption or desorption process.

Water state and distribution during fibre materials desorption process

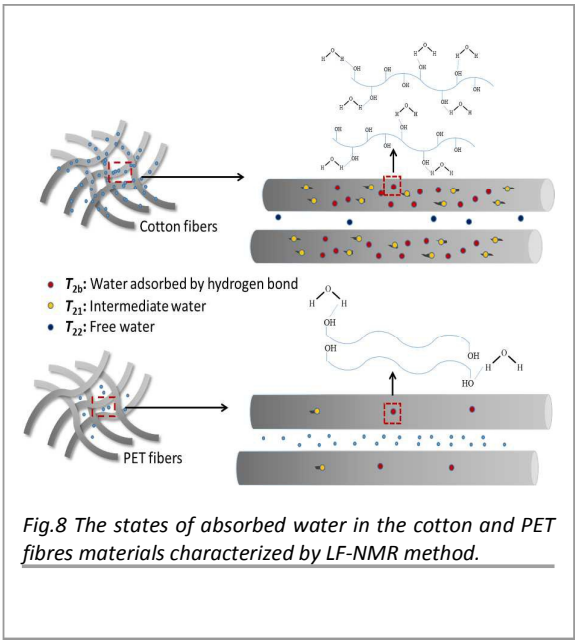

Fig.8 The states of absorbed water in the cotton and PET fibres materials characterized by LF-NMR method.

There are three different water states in the cotton and PET fibre materials from above study (shown in *Figure.8*). It is also worthy for us to investigate the mechanism of water state and distribution during desorption process of the fibre materials. The signal amplitude of different states of adsorbed water in fibre materials during water desorption process are shown in *Figure.9, T_{2b}, T_{21}* and T_{22} decreased. During desorption process of cotton fibre or PET fibre materials, it is most easily for bulk water (T_{22}) to desorb from fibre materials matrix. When the bulk water amount decrease, T_{21} becomes much shorter, since intermediate water interact with water hydrogen bonding with or the hydroxyl sites on polymer surface[42]. The decrease of T_{21} of absorbed water by microporous structure also has great effect on T_{2b} adsorbed by hydrogen bond, leading the decrease of T_{2b}[43]. The relaxation time further indicates the mechanism of water in fibre materials during desorption process. Three types of water in the fibre materials work together to present the time-domain spectra, where three peaks are really related each other. During desorption process of fibre materials, it is possible for the microstructure of fibre materials and water in the system to change. When the water is adsorbed by fibre materials, the mobility of water could chang. On the other hand, the interaction between water and fibre materials could have great influence on the property of fibre materials, such as swelling

phenomenon[44].

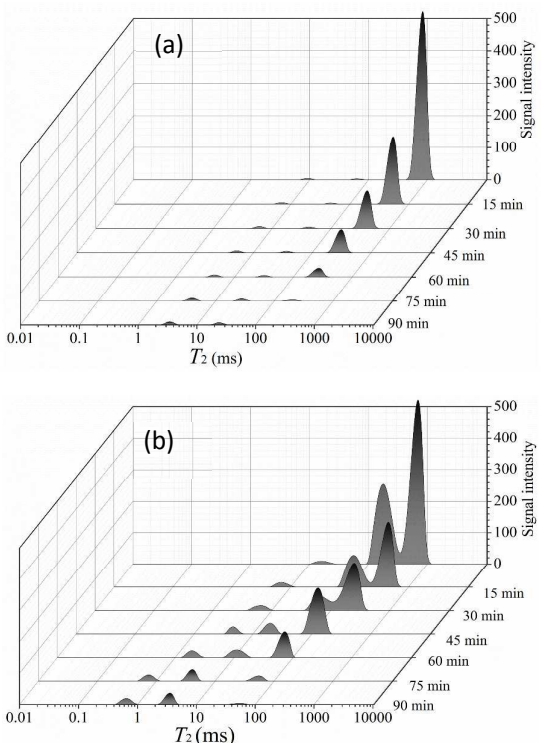

Fig.9 The signal amplitude and relaxation time of different adsorbed water in fibre materials during desorption process. (a) PET fibre materials; (b) Cotton fibre materials

LF-NMR provides unique insight into the water state and distribution during water desorption process. Above all the mechanism of the state and distribution of adsorbed water in the fibre materials, the relationship between the relaxations time (interaction) and desorption capacity was provided. Table.2 shows the measurement of relaxation time and desorption capacity of water adsorbed by chemical group, microporous and bulk water. The relaxation times 1-50 ms, 100-500 ms, 500-1500 ms of water adsorbed by chemical group, microporous structure and bulk water respectively. The order of desorption capacity of multiple structures is at T_{22}>T_{21}>T_{2b}. The results can provide the information that helps us to construct the ideal comfort clothing. Ideal clothing materials should thus have a high water retention capacity and high water transportation properties to maintain a constant temperature and humidity between skin and fabric when the human body is in a state of movement or hot environment.

The construction of fast adsorption and desorption of fibre materials

Table.2 The relaxation time of interaction of fibre materials

Adsorption structure	Adsorbed water	Interaction (KJ/mol)	T_2 (ms)
Chemical group	T_{2b}	12.6-29.3	1-50
Microporous structure	T_{21}	4.2-8.4	100-500
Bulk water	T_{22}	<2	500-1500

Comfortable clothe always absorbs moisture from atmospheres of greater humidity and releases it to a drier environment so as to create a balance in moisture conditions. In summer it is hot, and the fabrics for clothing are normally light, thin, and ventilated to make the wearer feel cool and comfortable. The human body tends to sweat, causing a moisture gradient from the human skin to the surrounding outdoor environment.

Based on the relationship between the interactions and desorption capacity, the fibre materials should have good wetting behavior and water retention capacity (water adsorbed at T_{21} and T_{22}) to reach the goal of fast adsorption-desorption process between fabrics and skin. Thus the design and study of comfortable fibre materials with liquid water moisture management properties is necessary to meet the requirements under these circumstances. Cotton fibre has higher water absorbency (water adsorbed at T_{2b} and T_{21}) than synthetic fibres such as PET fibre while the desorption capacity of PET fibre is better than that of cotton fibre. In this experiment PET fibre materials were chosen to further study. Firstly, PEG was used the chemical copolymerization modifier to improve the PET fibre wetting behavior. PETG copolymers with PEG of molecular weight from 800 to 20000 g/mol were synthesized by melt macromolecular interesterification method and then the PETG copolymers were molten spinning to get the PETG fibres. Figure10 shows the surface wetting behavior of PETG fibres. With the molecular weight of PEG increasing, the wetting behavior of PETG fibres increased. PETG fibre with the molecular weight 2000 g/mol of PEG was used to the next experiment. The hydrophilic property results of fibre materials reflects the nature of materials, but for comfortable clothes, comprehensive properties of fabric should be as the object to be further considered. It is necessary for us to investigate the fabrics designed by these fibre materials.

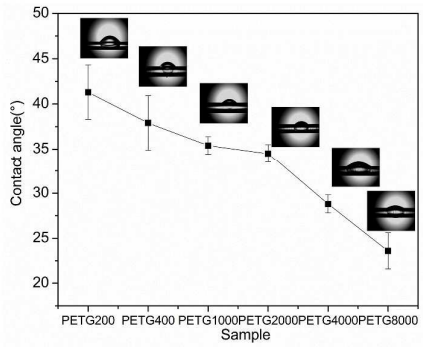

Fig.10 The surface wetting behavior of PETG fibres with different molecular weight of PEG from 200-8000 g/mol.
(a)0.1 mol/L; (b)0.2 mol/L; (c)0.4 mol/L; (d)0.8 mol/L;

Figure.11 shows the surface wetting behavior of PETG (shown in Figure11.a) and PET fabrics (shown in Figure11.b). When the water drop contacts with PETG fabrics, it can be immediately adsorbed into fabrics and the result of surface contact angle is about zero. At the condition of same designed structure of fabrics, PETG fabrics shows greater wetting behaviors compared with that of PET fabrics. Compared with untreated of PET fabrics, the wetting behavior of PET after treatment of hydrophilic finishing agent is more superior. The treatment of hydrophilic finishing agent of fabrics has been as

the most acceptable method to improve water adsorption capacity. But this method has poor wash resistance that the surface hydrophilic property decreased significantly due to the loss of finishing agent[45-46].

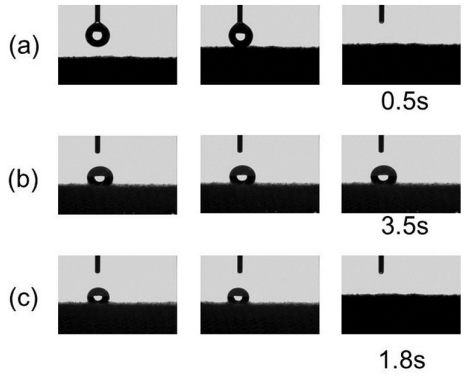

Fig.11 The surface wetting behavior of fabrics
(a) PETG fabrics; (b) PET fabrics; (c) PET fabrics after treatment of hydrophilic finishing agent

The surface wetting behavior of fabrics reaches the first step of fast adsorption-desorption process, the water adsorption capacity of fabrics will be further studied. The states of adsorbed water in the fibre materials has been investigated above. The water content adsorbed by microporous structure should be increased to satisfy a high water retention capacity to maintain a constant temperature and humidity between skin and fabric when the human body is in a state of movement or hot environment. The PETG and PET fibres were designed to the cross shaped structure to have a microstructure. The signal amplitude and relaxation time of different adsorbed water in fibre with cross shaped structure is shown in Figure.12. The cross-structure of PET and PETG fibre materials leads the T_{22} water increase significantly due to the microstructure adsorption capacity. Besides that the T_{2b} bound water content of PETG fabrics is higher than that of PET fabrics. This is caused the introduction of chemical group -O- of PEG into molecule, improving the number of hydrogen bond.

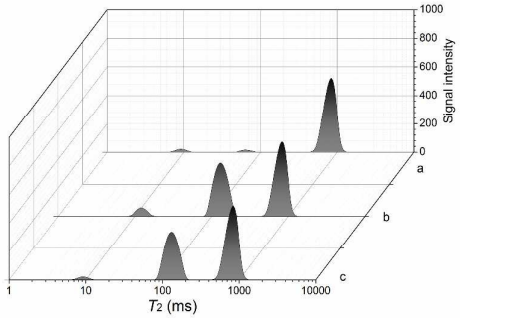

Fig.12 The signal amplitude and relaxation time of different adsorbed water in fibres with cross-shaped structure.
(a) PET fabrics; (b) PETG fabrics designed by cross-shaped structure fibre materials; (c) PET fabrics designed by cross-shaped structure fibre materials

Table3. The water adsorption and desorption date of PET and PETG fabrics

Samples	MA (%)	WAC (%)	Wicking distance(cm)	Diffusion time (s)
PETG	1.2	125	24	<0.5
PET	0.4	120	20	>3.0
a-PET	0.5	120	22	1.8
PETG*	1.2	125	24	<0.5
PET*	0.4	120	20	>3.0
a-PET*	0.4	120	20	>3.0

*represents the fabrics after water wash 10 times

Table3 shows the comprehensive evaluation adsorption and desorption properties of fabrics, including the moisture adsorption (*MA*), water adsorption capacity (*WAC*), wicking distance, diffusion time. The results of *MA* and *WAC* measurement reflect the hydrophilic property and adsorption capacity. There is no difference of *WAC* between PET, PETG and PET after treatment due to microstructure adsorbed water and free water account for the major adsorbed water. The moisture adsorption of PETG fabrics is higher than that of PET because of hydrophilic group -O- in the fibre materials. The experiment date of wicking distance and diffusion time describes the water transport behavior. Though PET fabric after treatment has excellent water transport behavior, it decreases obviously after water wash 10 times. The water vapor permeability illuminates the water adsorbed by muti-structure fabrics the desorption property. PETG fabrics retains the fast desorption advantage of PET. It may be ascribed to the design of muti-structure of fibre materials and control of interaction between muti-structure and water.

Conclusions

There are three different states of adsorbed water in the fibre materials. The interaction between multiple structures and water is at the order of $T_{2b}>T_{21}>T_{22}$. The analysis of T_2 component with different states shows that there are three categories of water. The slowest fraction T_{22} can be assigned to the bulk water. The intermediate component T_{21} can be ascribed to microporous structure confined water. The fastest fraction, T_{2b}, can be assigned to the water molecules trapped by hydrogen bond owing to the chemical group. When the water is adsorbed by fibre materials, the mobility of water could chang. On the other hand, the interaction between water and fibre materials could have great influence on the property of fibre materials. Three types of water in the fibre materials work together to present the time-domain spectra, where three peaks are really related each other. Based on the interaction between muti-structure and water, PET fibre materials were chosen to investigate the adsorption and desorption behaviors designed by copolymerization and cross-shaped method. The experiments of surface contact angle of fibre and fabric, moisture adsorption, water adsorption, wicking distance and water vapor permeability were carried out. The results show that the designed PETG fabrics have fast adsorption-desorption capacity. LF-NMR provides unique insight into the water state and distribution of muti-structure of fibre materials.

Acknowledgements

This work was financially supported by the National Natural Science Foundation of China (61134009), National Basic Research Program of China (2011BAE05B00, 2013BAE01B02), and the Program for Innovative Research Team in University of Ministry of Education of China (IRT1221). We also think the technical support staff from Shanghai Niumag Corporation (Shanghai, China).

References

1 Y. Park and E. Kim, *J. Appl. Polym. Sci*., 2012, **126**, 151.
2 S. Okubayashi, U. J. Griesser and T. Bechtold, *Carbohyd. Polym*., 2004, **58**, 293.
3 J. Speijers, J. H. Stanton, G. R. S. Naylor, P. Ramankutty and D. Tester, *Text. Res. J*., 2015, **85**, 1167.
4 S. V. Mikhalovsky, V. M. Gun'ko, V. A. Bershtein, V. V. Turov, L. M. Egorova, C. Morvan and L. I. Mikhalovska, *RSC Adv*., 2012, **2**, 2868.
5 C. Ganser, P. Kreiml, R. Morak, F. Weber, O. Paris, R. Schennach and C. Teichert, *Cellulose*., 2015, **22**, 2777.
6 H. Haddad, M.A. Kobaisi, *Mater. Design*., 2013, **49**, 230.
7 Y. Takeshita, E. Becker, S. Sakata, T. Miwa and T. Sawada, *Polymer*., 2014, **55**, 2505.
8 H. Wang, Y. Liu, J. Zhang, T. Li, Z. Hu and Y. Yu, *RSC Adv*., 2015, **5**, 11358.
9 F. T. Peirce, *J. Text. I*., 1929, **20**, 133.
10 A. R. Urquhart and N. Eckersall, *J. Text. I*., 1930, **21**, 49.
11 W. R. Vieth and K. J. Sladek, *J. Colloid. Interf. Sci*., 1965, **20**, 1014.
12 G. Zografi, J. T. Carstensen, M. Kontny and F. Attarchi, *J. Pharm. Pharmacol*., 1983, **35**, 455.
13 H. Kitano, T. Mori, Y. Takeuchi, S. Tada, M. Gemmei-Ide, Y. Yokoyama and M. Tanaka, *Macromol. Biosci*., 2005, **5**, 314.
14 R. Bline, V. Rutar, I. Zupancic, A. Zidansek, G. Lahajnar and J. Slak, *Appl. Magn. Reson*., 1995, **9**, 193.
15 E. L. Perkins and W. J. Batchelor, *Carbohyd. Polym*., 2012, **87**, 361.
16 R. N. Ibbett, S. K. Christian and F. Mario, *Polymer*., 2014, **49**, 5013.
17 Y. Wang, J. Guan, N. Hawkins, D. Porter and Z. Shao, *Soft. Matter*., 2104, **10**, 6321.
18 T. Xu, Q. Wu, S. Chen and M. Denga, *RSC Adv*., 2015, **5**, 32902.
19 C. P. Brown, J. Macleod, H. Amenitsch, F. C. Nerin, H. S. Gill, A. J. Price, E. Traversa, S. Licoccia and F. Rosei, *Nanoscale.*, 2011, **3**, 3805.
20 C. Connor and M. M. Chadwick, *J. Mater. Sci*., 1996, **31**, 3871.
21 J. Bednarek and S. Schlick, *J. Phys. Chem. C*., 1991, **95**, 9940.
22 A. Célino, O. Gonçalves, F. Jacquemin and S. Fréour, *Carbohyd. Polym*., 2013, **101**, 163.
23 F. Volke, S. Eisenblatter and G. Klose, *BIOPHYS. J*., 1994, **67**, 1882.
24 P. S. Liua, Q. Chen, S. S. Wu, J. Shen and S. C. Lin, *J. Membrane. Sci*., 2010, **350**, 387.
25 S. Mondal, J. L. Hu and Z. Yong, *J. Membrane. Sci*., 2006, **2**, 280.
26 A. WATANABE, S. MORITA and Y. OZAKI, *Appl. Spectrosc*., 2006, **60**, 1054.
27 C. Rana, A. D. Wit, M. Martin and M. Mishra, *RSC Adv*., 2014, **4**, 34369.
28 J. Grooth, W. Ogieglo, W. M. Vos, M. Girones and K. Nijmeijer, *Eur. Polym. J*., 2014, **55**, 57.
29 W. Wang, Y. Jin and Z. Su, *J. Phys. Chem. B*., 2009, **113**, 15742.
30 Y. M. Jung, H. S. Shin, S. B. Kim and I. Noda, *Appl. Spectrosc*., 2002, **56**, 1562.
31 L. Li, Y. Chen and S. J. Li, *Appl. Spectrosc*., 2006, **60**, 392.
32 D. A. Prokhorov, G. V. Mikoulinskaia, N. V. Molochkov, V. N. Uversky and V. P. Kutyshenko, *RSC Adv*., 2015, **5**, 41040.
33 K. Aeberhardt, Q. D. Bui and V. Normand, *Biomacromolecules*., 2007, **8**, 1038.
34 A. Ladhari, H. B. Daly, H. Belhadjsalah, K. C. Cole and J. Denault, *Polym. Degrad. Stabil*., 2010, **4**, 95.
35 P. Ji, J. Jin, G. Ji, C. Wang and H. Wang, *Polym. Eng. Sci*., 2015, **55**, 2195.
36 J. Wu, Z. Wang, W. Lin and S. Chen, *Acta. Biomater*., 2013, **9**, 6414.
37 F. Dalitz, M. Cudaj, M. Maiwaldd and G. Guthausen, *Prog. Nucl. Mag. Res. Sp*., 2012, **60**, 52.
38 J. Wu and S. f. Chen, *Langmuir*., 2012, **28**, 2137.
39 J. Wu, W. Lin, Z. Wang and S. Chen, *Langmuir*., 2012, **28**, 7436.
40 H. Peng, G. Zheng,Y. Sunb and R. Wang, *RSC Adv*., 2015, **5**, 78172.
41 L. Y. Ling, N. Y. Fei, X. Feng, C. Y. Shao, and D. H. Wei, *Polym. Adv. Technol*., 2011, **11**, 22.
42 D. Topgaard and O. Söderman, *Langmuir*., 2001, **17**, 2694.
43 D. Topgaard and O. Söderman, *J. Phys. Chem. B.*, 2002, **106,** 11887.
44 P. Knöös and D. Topgaard, *Langmuir*., 2013, **29**, 13898.
45 A. A. Deschamps, D.W. Grijpma, and J. Feijen, *Polymer*., 2001, **23**,
46 I. Taniguchi, S. Duan, T. Kai, S. Kazama, and H. Jinnai, *J. Mater. Chem. A*., 2013, **1**, 46.

